

Self-similar solutions for imploding z-pinch shells in magnetized plasmas

Y. M. SHTEMLER and M. MOND

Pearlstone Center for Aeronautical Engineering Studies,
Department of Mechanical Engineering, Ben-Gurion University of the Negev,
PO Box 653, Beer-Sheva 84105, Israel
(shtemler@bgu.ac.il, mond@bgu.ac.il, mondmichael@gmail.com)

(Received 9 July 2008 and accepted 22 January 2009, first published online
25 February 2009)

Abstract. Imploding z-pinch shells with total currents that are proportional to some power of time are investigated. Time-space separable self-similar solutions with cylindrical symmetry are explicitly obtained. The problem is treated asymptotically in high thermal conductivity within the model of magnetized resistive plasmas, while the ionization and radiation processes are ignored.

1. Introduction

Time-space separable self-similar quasi-equilibrium solutions are obtained for cylindrical z-pinch shells that implode under the pressure of an azimuthal magnetic field that is produced by the axial current.

Self-similar equilibrium solutions are of great interest due to their possible role as attractors at long times. Such solutions were previously found for full cylindrical z-pinch shells that carry total currents following a power law in time $\sim t^S$, with the pinch radius $\sim t^{(1-3S)/2}$. The z-pinch shells implode for $S > 1/3$ and explode otherwise (Bud'ko et al. 1994). The solutions are conventionally related to either exact (Coppins et al. (1988) for $S = \pm 1/3$) or long-time asymptotic (Bud'ko et al. (1994) for $S > -1/5$; see also Shtemler and Mond (2005), hereafter called SM 2005) mechanical equilibrium.

These studies were carried out within the framework of a resistive and heat conducting magneto-hydrodynamics (MHD) model. It was assumed that converting the magnetic energy into the kinetic energy of the z-pinch shells would add some dissipation and thereby the model of the resistive and thermally conductive plasma was adopted, while ionization and radiation effects that breaks the symmetry that underlies the self-similar solutions were neglected. Such solutions have been developed for two limiting cases of magnetized and unmagnetized plasmas (Coppins et al. 1988; Coppins et al. 1992; Bud'ko et al. 1994). In the case of a magnetized plasma, i.e. high values of $\Omega_{ci}\tau_{ii} \gtrsim 1$ (Ω_{ci} is the ion cyclotron frequency, τ_{ii} is the ion-ion collision time), explicit Bessel-type solutions were obtained in the limit of infinite thermal conductivity (isothermal approximation), which leaves the radius of the full z-pinch undetermined. In the limit of high but finite thermal conductivity, the ohmic heating and entropy terms are neglected in the leading-order energy equation; however, they are taken into account by the solvability condition for the next-order energy equation, and thus determine the pinch radius and influence the

leading-order approximate solution (SM 2005). A small parameter of the asymptotic procedure that is proportional to the square root of the electron-to-ion mass ratio naturally emerges in the magnetized plasma model. Explicit equilibrium solutions for high thermal conductivity significantly simplify the modeling compared with the limit of unmagnetized plasmas where the thermal conductivity is small (Coppins et al. 1992).

Although gas-puff z-pinchs are described in the limit of unmagnetized plasma rather than in the limit of magnetized plasmas (see also Sec. 6), the concept of the imploding shell observed in the gas-puff z-pinchs (Gregorian et al. 2003) forms the basis of the present study of quasi-equilibrium states in magnetized plasmas.

The recent experimental investigations of gas-puff z-pinchs (Gregorian et al. 2003, 2005a,b; Kroupp et al. 2007; see also the discussion in Sec. 6) refer to the model of annular z-pinch shell configurations, which differs from that for full cylindrical z-pinchs. The whole imploding phase may be separated into three stages: an initial stage that is characterized by a near-linear time variation of the total current and almost constant outer radius of the shell, an intermediate stage, and the final stagnation stage that corresponds to the saturation of the total current and the plasma converging at the pinch axis (Davara et al. 1998). At the final stagnation stage of the implosion the total mass of the imploding plasma significantly increases, the kinetic plasma energy is converted into plasma internal energy, and radiation is accompanied by shock waves and MHD turbulence (Gregorian et al. 2005a,b; Kroupp et al. 2007). During the intermediate stage, the imploding shell is characterized by a density that is significantly higher than in the dilute plasma in the inner region as well as by the highest radial velocities of the plasma, since the magnetic field energy is mainly spent on the radial flow. Although the inner ionization front propagates inward to the center of the pinch and ionizes the new portion of the working gas, the plasma mass rise is small, being only $\sim 10\%$, during the intermediate time interval. Thus, during this time the sweeping effect is small and the plasma column that contains most of the plasma mass has a nearly annular geometry. That annular region of the z-pinch plasma was named the ‘imploding shell’ by Gregorian et al. (2003), a term that is adopted hereafter.

In the present modeling the previous study of quasi-equilibrium self-similar solutions for full z-pinchs (SM 2005) is generalized to include z-pinch shells. As stated before, ionization and radiation processes as well as shock wave and sweeping effects are ignored. Instead, based on the concept of the imploding shell, an effective inner boundary of the imploding shell is introduced which satisfies the conventional kinematic and dynamic boundary conditions. The imploding shell concept of the quasi-equilibrium z-pinch is proposed as an alternative model to the full z-pinch model.

The quasi-equilibrium solutions of the MHD model which depend only on time and radius are also exact solutions of the Hall MHD model since in such cases the Hall term in Ohm’s law is identically zero. In this respect they may serve as basic states for studying the stability of Hall MHD plasmas, similar to the procedure for the full cylindrical z-pinchs (see e.g. Shtemler and Mond 2006 and references therein). The stability analysis is motivated by some experimental observations (see the discussion in Sec. 6) that demonstrate small-scale turbulent ion motion in the outer radius of the z-pinchs. The characteristic length scale of that turbulence may be compared with the wavelengths λ_H of the perturbations excited due to the

Hall electric field:

$$\lambda_H = \frac{c}{\omega_{pi}} = \frac{c}{2eZ} \sqrt{\frac{m_i}{\pi \hat{n}_i}} \sim 0.1 \text{ cm}, \tag{1.1}$$

where c is the light velocity, ω_{pi} is the ion plasma frequency, the ion current density averaged over the shell radius $\hat{n}_i \sim 10^{16} \text{ cm}^{-3}$ and the average ion charge $Z = 2$.

This paper is organized as follows. In the next section the basic governing relations are presented. Self-similar quasi-equilibrium solutions for z-pinch plasma shells are described in Sec. 3. In Sec. 4 asymptotic expansions in the limit of high thermal conductivity are carried out. Results of numerical simulations for the imploding shells are presented in Sec. 5. Applicability of the model of magnetized plasmas to conditions of gas-puff z-pinch, and the Hall instability within them, is discussed in Sec. 6. The principle results and conclusions of the study are given in Sec. 7. A closure condition that determines the outer radius of the pinch shell is derived in Appendix A. Explicit solution of the problem is carried out in Appendix B.

2. Governing relations

2.1. The physical model

A resistive MHD model for a quasi-neutral magnetized plasma that accounts for thermal conductivity is considered. The displacement current, viscosity, ionization, and radiation shock wave as well as sweeping effects are neglected:

$$\frac{\partial n}{\partial t} + \nabla(n\mathbf{V}) = 0, \tag{2.1a}$$

$$m_i n \frac{D\mathbf{V}}{Dt} = -\nabla P + \frac{1}{c} \mathbf{j} \times \mathbf{B}, \tag{2.1b}$$

$$\frac{1}{\gamma - 1} n^\gamma \frac{D}{Dt} (P n^{-\gamma}) = \eta_\perp j^2 - \nabla \cdot \mathbf{Q}, \quad \mathbf{Q} = -K_\perp \nabla T, \tag{2.1c}$$

$$P = 2nT, \tag{2.1d}$$

$$\mathbf{j} = \frac{1}{4\pi} c \nabla \times \mathbf{B}, \tag{2.1e}$$

$$\frac{\partial \mathbf{B}}{\partial t} + c \nabla \times \mathbf{E} = 0, \quad \nabla \cdot \mathbf{B} = 0, \quad \mathbf{E} = \eta_\perp \mathbf{j} - \frac{1}{c} \mathbf{V} \times \mathbf{B}. \tag{2.1f}$$

Here \mathbf{V} , $T = T_i = T_e$, and $P = P_e + P_i$ are the plasma velocity, temperature, and pressure. $P_k = n_k T_k$, m_k are the electron and ion masses, where $k = e, i$, $n \approx n_i = n_e/Z$ is the number density, Z is the effective ion charge of the quasi-neutral plasma, $\gamma = 5/3$ is the specific heat ratio, \mathbf{B} and \mathbf{E} are the magnetic and electric fields, \mathbf{j} is the current density, c is the speed of light, $D/Dt = \partial/\partial t + (\mathbf{V} \cdot \nabla)$, t is the time and \mathbf{Q} is the ion heat flux. η_\perp and K_\perp are the cross-field Spitzer resistivity and ion thermal conductivity (Lifshits and Pitaevskii 1981),

$$K_\perp = \frac{a_i n^2}{B^2 T^{1/2}}, \quad \eta_\perp = \frac{a_e}{T^{3/2}},$$

$$a_i = aZ^2 e^2 c^2 \sqrt{m_i}, \quad a_e = aZe^2 \sqrt{m_e/2}, \quad a = \frac{8}{3} l \sqrt{\pi},$$

where $l \approx 14$ is the Coulomb logarithm, e is the electron charge and, for magnetized plasmas,

$$\Omega_{ci}\tau_{ii} \gg 1, \quad \Omega_{ci} = \frac{ZeB}{m_i c}, \quad \tau_{ii} = \frac{m_i^{1/2} T^{3/2}}{4\pi Z^4 e^4 l n}. \tag{2.2}$$

The physical system is described in a cylindrical frame of reference (r, θ, z) , where subscripts $r, \theta,$ and z denote the corresponding projections. The boundary conditions for the thermally isolated z-pinch shell for vanishing sheet currents are as follows (Kruskal and Schwarzschild 1954):

$$P = 0, \quad V_r = V_{out}, \quad Q_r = 0, \quad B_\theta = B_{out} \quad \text{at } r = r_{out}, \tag{2.3a}$$

$$V_r = V_{in}, \quad Q_r = 0, \quad B_\theta = 0 \quad \text{at } r = r_{in}. \tag{2.3b}$$

Here r_k and V_k are the pinch radius and boundary velocity for the outer and inner edges, $k = out, in$. Outside the pinch the toroidal magnetic field is potential one:

$$B_{out}(r, t) = \frac{2I(t)}{cr} \quad \text{at } r \geq r_{out}. \tag{2.4}$$

The system of relations (2.1)–(2.4) is complemented by the integral conditions for the total current, $I(t)$, that is a known function of time, and for the constant line density, N , of the imploding shell:

$$2\pi \int_{r_{in}}^{r_{out}} j_z r \, dr = I(t), \quad 2\pi \int_{r_{in}}^{r_{out}} nr \, dr = N \equiv \text{const}. \tag{2.5}$$

Due to Ampère’s law in (2.1) and relation (2.4), relation (2.5) for the total current is satisfied identically and is omitted from further consideration. The initial data is not relevant here since time-space separable self-similar solutions are sought.

For equilibrium cylindrical z-pinch shells, the Bennett relation for the temperature averaged over the pinch-shell cross-section, T_B , follows from the equilibrium momentum equation (i.e. with zero acceleration) and Ampère’s law

$$T_B(t) = T_{max}(t) - \frac{\pi r_{in}^2(t) P_{in}(t)}{(1 + Z)N}, \quad T_{max}(t) = \frac{I^2(t)}{2(1 + Z)c^2 N}.$$

Here T_{max} is the Bennett mean temperature for the associated full cylindrical z-pinch at zero pressure $P_{in} = P(r_{in})$ at the inner edge. The Bennett relation is used for verifying the numerical solution.

2.2. Dimensionless equations

All relevant characteristic normalizing scales denoted by subscript * may be expressed through four independent scales, namely, the characteristic radius and time (r_*, t_*) as well as the given dimensional line density N and total current I_* :

$$m_* = m_i, \quad V_* = \frac{r_*}{t_*}, \quad T_* = \frac{I_*^2}{c^2 N}, \quad n_* = \frac{N}{r_*^2}, \quad j_* = \frac{I_*}{r_*^2}, \quad P_* = n_* T_*, \tag{2.6}$$

$$B_* = \frac{I_*}{cr_*}, \quad E_* = \frac{r_* B_*}{ct_*}, \quad \eta_* = \frac{a_e}{T_*^{3/2}}, \quad K_* = \frac{a_i P_*^2}{T_*^{5/2} B_*^2}, \quad Q_* = \frac{a_i P_*^2}{T_*^{3/2} B_*^2 r_*}.$$

Substituting (2.6) into (2.1)–(2.5) results in

$$\frac{\partial n}{\partial t} + \frac{1}{r} \frac{\partial}{\partial r}(rnV_r) = 0, \tag{2.7a}$$

$$\Pi_i n \left(\frac{\partial V_r}{\partial t} + V_r \frac{\partial V_r}{\partial r} \right) = -\frac{\partial P}{\partial r} - j_z B_\theta, \tag{2.7b}$$

$$\frac{1}{\gamma - 1} n^\gamma \left[\frac{\partial}{\partial t}(Pn^{-\gamma}) + V_r \frac{\partial}{\partial r}(Pn^{-\gamma}) \right] = \Pi_R \eta_\perp j_z^2 - \Pi_T \frac{1}{r} \frac{\partial}{\partial r}(rQ_r), \tag{2.7c}$$

$$P = (1 + Z)n\eta_\perp^{-2/3}, \tag{2.7d}$$

$$j_z = \frac{1}{4\pi r} \frac{\partial}{\partial r}(rB_\theta), \tag{2.7e}$$

$$\frac{\partial B_\theta}{\partial t} - \frac{\partial}{\partial r}(\Pi_R \eta_\perp j_z - V_r B_\theta) = 0. \tag{2.7f}$$

Here the temperature and the radial heat flux are expressed through the resistivity

$$T = \eta_\perp^{-2/3}, \quad Q_r = \frac{2P^2}{3(1 + Z)^2 B^2} \frac{\partial \eta_\perp}{\partial r}.$$

The dimensionless boundary conditions at the pinch edges, the integral mass conservation law, and the condition for magnetized plasmas are given by

$$V_r = V_{\text{out}}, \quad B_\theta = \frac{2I(t)}{r}, \quad Q_r = 0, \quad P = 0, \quad \text{at } r = r_{\text{out}}, \tag{2.8a}$$

$$V_r = V_{\text{in}}, \quad B_\theta = 0, \quad Q_r = 0 \quad \text{at } r = r_{\text{in}}, \tag{2.8b}$$

$$2\pi \int_{r_{\text{in}}}^{r_{\text{out}}} nr \, dr = 1, \tag{2.8c}$$

$$\Omega_{\text{ci}} \tau_{\text{ii}} \sim \Pi_{\text{M}} \gg 1. \tag{2.8d}$$

The dimensionless parameters in relations (2.7)–(2.8) are

$$\Pi_{\text{I}} = \frac{m_i r_*^2}{T_* t_*^2}, \quad \Pi_{\text{T}} = \frac{\Pi_{\text{R}}}{\epsilon}, \quad \Pi_{\text{R}} = \frac{t_* a Z^2 e^2 c^2 \sqrt{m_i}}{T_*^{3/2} r_*^2} \epsilon, \quad \Pi_{\text{M}} = \frac{2T_*^2 r_*}{3acZ^3 e^3 \sqrt{\pi N m_i}}, \tag{2.9}$$

where $\epsilon \lesssim 1$ is proportional to the square root of the electron-to-ion mass ratio

$$\epsilon = \frac{a_e c^2}{a_i} \equiv \frac{1}{Z} \left(\frac{m_e}{2m_i} \right)^{1/2}. \tag{2.10}$$

Alternatively, the inertial, heat-transfer and magnetization parameters Π_{I} , Π_{T} and Π_{M} may be expressed through the resistivity parameter Π_{R} and the Lundquist number Lu that is defined through the characteristic Alfvén speed V_a ,

$$\Pi_{\text{I}} = \frac{1}{\Pi_{\text{R}}^2 Lu^2}, \quad \Pi_{\text{T}} = \frac{\Pi_{\text{R}}}{\epsilon}, \quad \Pi_{\text{M}} = \epsilon Lu \Pi \quad \left(\Pi = \frac{2c}{3Ze} \sqrt{\frac{m_i}{\pi N}} \right), \tag{2.11a}$$

$$Lu = \frac{V_a r_*}{c^2 \eta_*} \equiv \frac{T_*^2 r_*}{c^2 a Z^2 e^2 m_i} \frac{1}{\epsilon} \quad \left(V_a = \frac{B_*}{\sqrt{m_i n_*}} \equiv \frac{T_*}{\sqrt{m_i}} \right). \tag{2.11b}$$

The condition for the plasma magnetization is $\Pi_M \gtrsim 1$. The quasi-equilibrium state is reached if the inertial term in the momentum equation is small, i.e. $\Pi_I \gtrsim 1$. That condition presumes that the characteristic time t_* , during which the equilibrium self-similar solution settles, is smaller than the current pulse duration of the imploding z-pinch shell. Since the current pulse duration is bounded from above, the latter condition essentially restricts the admissible values of the z-pinch parameters consistent with the solution developed in the present study: the equilibrium self-similar isothermal solution should be settled during the life-time of the z-pinch. Note also that the condition for applicability of the isothermal approximation is $\Pi_T \gtrsim 1$. According to (2.11a) all the above three conditions ($\Pi_I \gtrsim 1$, $\Pi_T \gtrsim 1$ and $\Pi_M \gtrsim 1$) are satisfied if

$$Lu \gtrsim \epsilon^{-1}, \quad \Pi_R \gtrsim \epsilon. \tag{2.12}$$

3. Self-similar solutions

For cylindrical z-pinch shells, the same self-similarity law is valid as for conventional full cylindrical z-pinch (Bud'ko et al. 1994; see also SM 2005):

$$\begin{aligned} t &= \tilde{t}, \quad r = \tilde{r}\alpha(\tilde{t}), \quad V_r(r, t) = \tilde{r}\dot{\alpha}(\tilde{t}), \quad a_r(r, t) = \tilde{r}\ddot{\alpha}(\tilde{t}), \\ r_k(t) &= \tilde{r}_k\alpha(\tilde{t}), \quad V_k(t) = dr_k/dt, \quad a_k(t) = dV_k/dt, \\ I(t) &= \tilde{I}\tilde{t}^S, \quad j_z(r, t) = \tilde{j}(\tilde{r})\alpha^{\kappa_1}(\tilde{t}), \quad B_\theta(r, t) = \tilde{B}(\tilde{r})\alpha^{\kappa_2}(\tilde{t}), \\ T(r, t) &= \tilde{T}(\tilde{r})\alpha^{\kappa_3}(\tilde{t}), \quad P(r, t) = \tilde{P}(\tilde{r})\alpha^{\kappa_4}(\tilde{t}), \\ \eta_\perp(r, t) &= \tilde{\eta}(\tilde{r})\alpha^{\kappa_5}, \quad n(r, t) = \tilde{n}(\tilde{r})\alpha^{\kappa_6}(\tilde{t}), \quad Q_r(r, t) = \tilde{Q}(\tilde{r})\alpha^{\kappa_7}(\tilde{t}). \end{aligned} \tag{3.1}$$

Here $a_r(r, t) = DV_r(r, t)/Dt$ is the plasma acceleration, $a_k(t)$ is the pinch boundary acceleration, $\tilde{r}_k \equiv \text{const}$, $k = \text{in, out}$, $\alpha(\tilde{t}) = \tilde{t}^{\kappa_0}$, the upper dots denote the derivatives of $\alpha(\tilde{t})$ with respect to time \tilde{t} and

$$\begin{aligned} \kappa_0 &= \frac{1 - 3S}{2}, \quad \kappa_1 = \frac{4S - 1}{\kappa_0}, \quad \kappa_2 = \frac{5S - 1}{2\kappa_0}, \quad \kappa_3 = \frac{2S}{\kappa_0}, \\ \kappa_4 &= \frac{5S - 1}{\kappa_0}, \quad \kappa_5 = -\frac{3S}{\kappa_0}, \quad \kappa_6 = \frac{3S - 1}{\kappa_0}, \quad \kappa_7 = \frac{7S - 3}{2\kappa_0}. \end{aligned} \tag{3.2}$$

In the present study we focus on imploding z-pinch shells with total current exponent $S > 1/3$. The arbitrary dimensionless total current amplitude \tilde{I} in relations (3.1) may be set to unity ($\tilde{I} = 1$) due to the choice of the characteristic total-current amplitude I_* . However, a more convenient choice of I_* is used in Sec. 5.

Substituting (3.1)–(3.2) into (2.7) results in

$$0 = \frac{d\tilde{P}}{d\tilde{r}} + \tilde{j}\tilde{B}, \tag{3.3a}$$

$$\frac{d\tilde{\eta}}{d\tilde{r}} = \epsilon \frac{3(1 + Z)^2 \tilde{B}^2}{2\tilde{r} \tilde{P}^2} \int_0^{\tilde{r}} \tilde{r} \left(\tilde{\eta}\tilde{j}^2 - \frac{\Gamma}{\Pi_R} \tilde{P} \right) d\tilde{r} \quad \left(\tilde{Q} = \frac{2}{3(1 + Z)^2} \frac{\tilde{P}^2}{\tilde{B}^2} \frac{d\tilde{\eta}}{d\tilde{r}} \right), \tag{3.3b}$$

$$(1 + Z)\tilde{n} = \tilde{P}\tilde{\eta}^{2/3} \quad (\tilde{T} = \tilde{\eta}^{-2/3}), \tag{3.3c}$$

$$\tilde{j} = \frac{1}{4\pi\tilde{r}} \frac{d}{d\tilde{r}}(\tilde{r}\tilde{B}), \tag{3.3d}$$

$$S\tilde{B} - \Pi_R \frac{d}{d\tilde{r}}(\tilde{\eta}\tilde{j}) = 0. \tag{3.3e}$$

Here $\Gamma = 1 + 3S(\gamma - 5/3)/(\gamma - 1)$ so that $\Gamma = 1$ everywhere below for $\gamma = 5/3$.

The kinematic boundary conditions and the mass balance relations (2.8) are satisfied identically for the solution (3.1), while the rest of the boundary conditions at the pinch edges and the integral condition for the line density are

$$\tilde{B} = 0, \quad \tilde{P} = 0, \quad \tilde{Q} = 0 \quad \text{at } \tilde{r} = \tilde{r}_{\text{out}}, \tag{3.4a}$$

$$\tilde{B} = 0, \quad \tilde{Q} = 0 \quad \text{at } \tilde{r} = \tilde{r}_{\text{in}}, \tag{3.4b}$$

$$\pi\tilde{\eta}^{2/3} \int_{\tilde{r}_{\text{in}}}^{\tilde{r}_{\text{out}}} \tilde{P}\tilde{r} d\tilde{r} = (1 + Z)/2. \tag{3.4c}$$

4. High-thermal-conductivity asymptotic expansions

Further simplifications are still possible in the problem described in (3.3)–(3.4), which contain the small parameter ϵ . Thus solutions of (3.3)–(3.4) are sought in the limit of high thermal conductivity in the form of a power series in ϵ (SM 2005):

$$\tilde{f}(\tilde{r}) = f^{(0)}(\rho) + \epsilon f^{(1)}(\rho) + \dots, \quad \rho_k = \rho_k^{(0)} + \epsilon \rho_k^{(1)} + \dots, \tag{4.1a}$$

$$\rho = \tilde{r}/\lambda, \quad \rho_k = \tilde{r}_k/\lambda \quad (k = \text{in}, \text{out}), \tag{4.1b}$$

where $\tilde{f}(\tilde{r})$ stands for any of the unknown functions; the new independent variable ρ is scaled by an arbitrary positive constant λ that is determined below.

Substituting (4.1) into (3.3)–(3.4) yields, to leading order in ϵ (the mass balance equation is satisfied identically for the self-similar solutions),

$$\frac{dP}{d\rho} + \lambda j B = 0, \tag{4.2a}$$

$$\frac{d\eta}{d\rho} = 0, \tag{4.2b}$$

$$(1 + Z)n = P\eta^{2/3} \quad (T = \eta^{-2/3}), \tag{4.2c}$$

$$j = (4\pi\lambda\rho)^{-1} \frac{d}{d\rho}(\rho B), \tag{4.2d}$$

$$\lambda S B - \Pi_R \eta \frac{dj}{d\rho} = 0. \tag{4.2e}$$

The superscript denoting the approximation order with respect to ϵ is dropped everywhere in what follows unless this leads to misunderstanding.

The boundary conditions for the heat flux are identically satisfied in the isothermal approximation (4.2b), while the rest of the boundary conditions at the pinch edges and the integral condition for the line density are as follows:

$$B = 0 \quad \text{at } \rho = \rho_{\text{in}}, \quad B = 2/(\lambda\rho), \quad P = 0 \quad \text{at } \rho = \rho_{\text{out}}, \tag{4.3a}$$

$$\pi\lambda^2 \int_{\rho_{\text{in}}}^{\rho_{\text{out}}} n\rho d\rho = (1 + Z)/2. \tag{4.3b}$$

The differential equation for the magnetic field reduces to the standard form for Bessel functions for the value of λ chosen as follows:

$$\frac{d}{d\rho} \left[\frac{1}{\rho} \frac{d}{d\rho} (\rho B) \right] - B = 0, \quad (4.4a)$$

$$\lambda = \Lambda \sqrt{\eta}, \quad \Lambda = \frac{1}{2} \sqrt{\frac{\Pi_R}{\pi S}}. \quad (4.4b)$$

Using (4.3)–(4.4) yields the following general solution of the system (4.2):

$$T = C_0 \quad (\eta = C_0^{-3/2}), \quad (4.5a)$$

$$B = C_1 I_1(\rho) + C_2 K_1(\rho), \quad (4.5b)$$

$$j = \frac{1}{4\pi\lambda} [C_1 I_0(\rho) - C_2 K_0(\rho)], \quad (4.5c)$$

$$P + 2\pi\lambda^2 j^2 = \frac{1}{4\pi} C_3. \quad (4.5d)$$

Here $I_m(\rho)$ and $K_m(\rho)$ are the Bessel functions ($m = 0, 1$).

Four boundary conditions (4.3), closed by the solvability condition (A 2) for the energy equation in the first-order approximation in ϵ (see Appendix A), lead to an algebraic system of five equations for the six unknown variables, the coefficients C_j ($j = 0, 1, 2, 3$) together with the outer and inner radii of the pinch (or, equivalently, for the outer radius of the shell ρ_{out} and the radius ratio $A = \rho_{\text{in}}/\rho_{\text{out}}$). Thus, substituting (B 7)–(B 9) for the coefficients C_j ($j = 0, 1, 2, 3$) and the solution of the eigenvalue equation (B 6) for ρ_{out} vs A (Appendix B) into (4.5) provides explicit expressions for the radial profiles of all the relevant physical variables.

5. Results of numerical simulations for imploding z-pinch shells

5.1. Solution of the eigenvalue equation for the outer radius

The eigenvalue equation (B 6) in Appendix B that relates the outer and inner radii of the pinch shell, rewritten in terms of the outer radius ρ_{out} and the inner-to-outer radius ratio $A = \rho_{\text{in}}/\rho_{\text{out}}$, is

$$D(\rho_{\text{out}}, A; S) = 0. \quad (5.1)$$

In Fig. 1 the dependence of ρ_{out} on $A = \rho_{\text{in}}/\rho_{\text{out}}$ is depicted. It was obtained by the numerical solution of the eigenvalue equation for $S = 2.5$.

5.2. Characteristics of z-pinch shells for typical parameters of magnetized plasma

The following physical quantities are considered as the basic parameters that characterize the imploding z-pinch shell: the inner-to-outer radius ratio $A = \rho_{\text{in}}/\rho_{\text{out}}$, the line density N , the total-current exponent S , the constant value of the average ion charge Z , the constant temperature T , and the characteristic time and radius t_* and r_* . It is convenient here to fit a given temperature T by the choice of the characteristic total current I_* . The characteristic time t_* that is naturally associated with the time of equilibrium settling may be estimated by fitting the observed values of the total current or the outer radius to that in the self-similar solution, while the characteristic size is chosen to be equal to the shell thickness

$$r_* = (1 - A)r_{\text{out}}. \quad (5.2)$$

Table 1. Characteristics of the z-pinch shell for typical parameters of the plasma, $S = 2.5$, $A = 0.8$, $T = 0.25$ keV, $\rho_{out} \approx 17$, $t_* = 85$ ns, $\epsilon = 0.017/Z$, and $\Pi_T = \Pi_R/\epsilon$.

T (Z) (keV)(-)	$10^{-17}N$ (m^{-1})	I_* (kA)	r_{out} (cm)	P_{in} (MPa)	Π_R (-)	$10^5\Pi_I$ (-)	Π_M (-)	$10^{-3}Lu$ (-)	$10^{-16}\hat{n}$ (cm^{-3})	λ_H (cm)
3.1 1	0.25	11	0.17	0.7	0.13	2	50	1.6	0.75	0.26
3.1 1	0.5	16	0.17	1.5	0.13	2	35	1.6	1.5	0.18
3.1 1	1.0	22	0.17	2.9	0.13	2	25	1.6	3.0	0.13
4.7 2	0.25	14	0.24	0.5	0.06	4	22	2.7	0.3	0.2
4.7 2	0.5	19	0.24	1.1	0.06	4	15	2.7	0.62	0.15
4.7 2	1.0	27	0.24	2.2	0.06	4	11	2.7	1.25	0.1

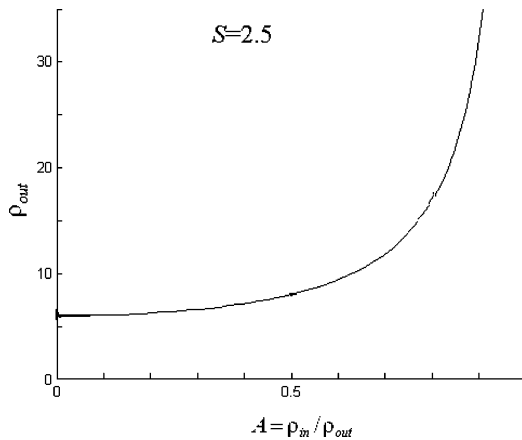


Figure 1. The outer radius of the imploding z-pinch shell ρ_{out} vs $A = 0.8$ ($S = 2.5$).

The outer radius is determined by relations (4.1b) and (4.4b):

$$\frac{r_{out}}{r_*} = \frac{1}{2} \sqrt{\frac{\Pi_R}{\pi S}} \frac{T^{3/4}}{T_*^{3/4}} \rho_{out}, \tag{5.3}$$

where T_* is determined in (2.6), and ρ_{out} is the solution of the eigenvalue equation (5.1). The dimensional outer radius r_{out} is independent of r_* , since the dimensionless resistivity parameter Π_R in (2.9) is proportional to $1/r_*^2$.

Characteristic results are presented in Table 1 in mixed SI–Gauss units for typical parameters of z-pinch plasmas for $t = t_*$. The dimensionless parameters of the model, Π_R , Π_I , Π_M , and Lu , may be calculated according to (2.9) and (2.11). It can be seen from Table 1 that the parameters of the imploding shell satisfy sufficiently well the conditions of the model applicability (2.12). Note that conditions (2.12) depend on only two determining parameters, namely, the Lundquist number Lu and the resistivity parameter Π_R . In turn the Lundquist number depends on the characteristic temperature and radius $Lu \sim T_*^2 r_*$, while the resistivity parameter depends additionally on the characteristic time, $\Pi_R \sim t_*/(T_*^{3/2} r_*^2)$. Hence, for any given characteristic radius r_* , the Lundquist number satisfies the first of (2.12) for sufficiently large T_* , while t_* is the principal parameter, whose value allows one to satisfy the second of conditions (2.12). Note also that for t_* larger than 85 ns adopted in Table 1 the resistivity parameter Π_R is larger and conditions (2.12) are better satisfied. The pressure at the inner edge $P_{in} = P(r_{in})$ and the characteristic

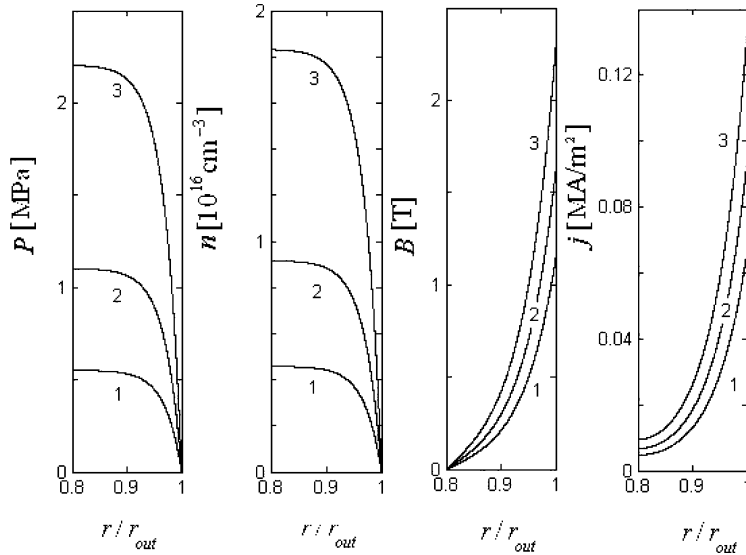


Figure 2. Dimensionless radial profiles of pressure, density, and magnetic and electric fields. $S = 2.5$, $Z = 2$, $A = 0.8$, $T = 0.25$ keV, $\Pi_R \approx 0.06$, $\Pi_I \approx 4 \times 10^{-5}$, $\Pi_M \approx 15$, $Lu \approx 2.7 \times 10^3$, $\epsilon \approx 8 \times 10^{-3}$ (see Table 1). Curves 1, 2, and 3 correspond to $N = 1 \times 10^{17}$ cm $^{-3}$, 2×10^{17} cm $^{-3}$, and 3×10^{16} cm $^{-3}$, respectively.

wavelengths of the perturbations excited in the Hall regime λ_H , calculated by using (1.1), are also presented in Table 1.

In Fig. 2 the radial profiles of the pressure, density, magnetic field, and electric current are depicted for typical parameters of z-pinch imploding shells. Note that the magnetic field and electric current have their maxima at the outer edge of the shell, while the maximum of the number density (pressure) is located at the effective inner edge.

6. Discussion

Annular gas-puff devices are characterized by a sufficiently large initial radius and the driving pulse width of the total current is comparable to the total implosion time. Although the duration of the whole process is too short to reach a Bennett-like mechanical equilibrium (Ryutov et al. 2000), the concept of the imploding shell by Gregorian et al. (2003) rather assumes that the shell is in equilibrium due to the small duration of the imploding shell stage compared to the total implosion time, and the thin shell thickness compared with the entire thickness of the plasma shell.

The gas-puff device discussed in Gregorian et al. (2003) produces an annular shell of the working gas (CO $_2$). The total duration of the implosion is ~ 620 ns, while the duration of the imploding shell stage is from 100 ns from 435 ns to 535 ns (Fig. 1(b) in Gregorian et al. (2003)). At this period, the outer boundary of the plasma shell moves radially from $r_{out} \approx 2$ cm to $r_{out} \approx 1.1$ cm, the thickness of the imploding shell during this period is $r_{out} - r_{in} \approx (0.1-0.15)$ cm ± 0.1 cm wide, while the entire plasma shell is about 0.6 cm wide. Then, the following characteristic scales may be adopted: the time instant of the start of the imploding shell stage $t_* = t_1 \approx 435$ ns, the ratio of the inner-to-outer radius $A = r_{in}/r_{out} \approx 0.9$ cm, and the mean thickness

of the imploding shell $r_* = r_{\text{out}} - r_{\text{in}} \approx 0.125$ cm. Furthermore, during that time the total current does not exceed the value I_{max} (see Fig. 1 in Davara et al. (1998)): $I_* < I_{\text{max}} < 175$ kA. Since the imploding shell is charged with the ionization degree $Z \sim 3\text{--}4$ (see Fig. 7 in Gregorian et al. (2005a)), the effective value $Z \approx 4$ may be adopted. The dimensional line density of the imploding plasma in those experiments is $N_w \approx (10 \pm 3) \mu\text{g}/\text{cm}$ for CO_2 gas (reduced to 70% of the imploding shell mass this yields $0.7 \cdot (10 \pm 3) \mu\text{g}/\text{cm}$) or, equivalently,

$$N = \frac{N_w [\mu\text{g}/\text{cm}]}{N_{\text{CO}_2} m_i [\mu\text{g}]} \sim 10^{17} \text{ cm}^{-1},$$

where N_{CO_2} is the particle number in one molecule of CO_2 . The average value of the electron number density observed in the experiments (see Fig. 5(b) in Gregorian et al. (2003)) is $\hat{n}_e = Z\hat{n}_i \sim 4 \times 10^{17} \text{ cm}^{-3}$, which yields $\hat{n}_i \sim 1 \times 10^{17} \text{ cm}^{-3}$.

The above estimations for I_{max} , N , r_* , and Z yield the following value for the magnetization parameter (using the expression for T_* through I_* in (2.6)):

$$\Pi_M = \frac{2T_*^2 r_*}{3acZ^3 e^3 \sqrt{\pi N m_i}} \equiv \frac{2I_*^4 r_*}{3ac^5 Z^3 e^3 N^{5/2} \sqrt{\pi m_i}} < \frac{2I_{\text{max}}^4 r_*}{3ac^5 Z^3 e^3 N^{5/2} \sqrt{\pi m_i}} \approx 0.06.$$

Thus, the plasma magnetization condition $\Pi_M \gtrsim 1$ is violated, and the limit of unmagnetized plasma is rather applicable to the experimental conditions in Gregorian et al. (2003). Note also that the estimation $\Pi_M \sim 0.06$ is also valid for the case of unmagnetized plasma, since the magnetization condition has the same form as for magnetized plasma up to a constant factor of the order of unity (Coppins et al. 1992).

Experiments by Gregorian et al. (2005a) exhibit small-scale turbulent ion motion in the outer radius of the z-pinch shell with wavelength $\lambda \sim c/\omega_{\text{pi}} < 0.05$ cm. Such small scale perturbations may be excited by the Hall instability. Indeed, adopting the above estimations \hat{n}_i and Z yield $\lambda_H = c/\omega_{\text{pi}} \sim 0.02$ cm for the wavelength excited in the Hall regime (see (1.1)).

7. Summary and conclusions

Time-separable self-similar quasi-equilibrium solutions were developed. The concept of the imploding shell proposed by Gregorian et al. (2003) for interpretation of the experimental data for gas-puff z-pinches in unmagnetized plasmas lies in the basis of the present modeling of z-pinches in magnetized resistive plasmas. The intermediate time interval of the implosion corresponds to the imploding shell stage during which the radiation and ionization processes as well as shock wave and sweeping effects are ignored.

The problem is treated asymptotically in the limit of high, but finite, thermal conductivity (similar to the full cylindrical z-pinches, SM 2005). The resulting characteristics of the quasi-equilibrium z-pinch shells are determined by the following input values: the ion charge Z , the ratio of the inner-to-outer radius A , the total current exponent S , the line density N , and the constant temperature T , as well as the characteristic settling time of the equilibrium t_* (the characteristic length r_* is chosen to be equal to the shell thickness). The model determines the outer radius of the shell, while the inner shell radius is known up to an arbitrary factor. The radial profiles of the magnetic and electric fields, pressure, density etc. are calculated for typical parameters of the plasmas. Considering the comparison of the present

qualitative modeling with the results of experiments or numerical computations, the outer interface of the model must be associated with the location of the magnetic field maximum that separates the plasma from the surroundings, while the effective inner boundary of the imploding shell should be associated with the location of the density (pressure) maximum. Estimations have been made which demonstrate the possibility of the Hall instability for typical plasma parameters.

Appendix A. Closure condition

Following SM 2005, the boundary conditions (4.3) are closed by considering the first-order approximation in ϵ of the energy equation (3.3b):

$$\frac{d\eta^{(1)}}{d\rho} = \frac{3(1+Z)^2}{2} Q^{(1)}(\rho) \frac{B^2(\rho)}{P^2(\rho)}, \quad Q^{(1)}(\rho) = \frac{1}{\rho} \int_{\rho_{\text{in}}}^{\rho} \rho \left[\eta j^2(\rho) - \frac{\Gamma}{\Pi_R} P(\rho) \right] d\rho. \quad (\text{A } 1)$$

Here P and B are given by the zero-order approximation in ϵ , and as above the superscript 0 is omitted with no misunderstanding, but superscript 1 for the first-order approximation is preserved with no confusion.

According to the boundary conditions, at the outer pinch edge in (4.3a) the pressure is zero, while the magnetic field there is non-zero, $P(\rho_{\text{out}}) = 0$, $B(\rho_{\text{out}}) \neq 0$. As a result, (A 1) is singular at $\rho = \rho_{\text{out}}$ for $Q^{(1)}(\rho_{\text{out}}) \neq 0$. Hence, the coefficient $Q^{(1)}(\rho)$ must vanish at $\rho = \rho_{\text{out}}$ in order to avoid that singularity (SM 2005):

$$\int_{\rho_{\text{in}}}^{\rho_{\text{out}}} \rho [\Gamma P(\rho) - \Pi_R \eta j^2(\rho)] d\rho = 0. \quad (\text{A } 2)$$

Let us reduce the closure condition (A 2) to an equivalent but more convenient form. Multiplying (4.5d) by $2S\rho$, using the definition of $\lambda = \Lambda\sqrt{\eta}$ in (4.4b) and integrating the result over the pinch radius from ρ_{in} to ρ_{out} yields

$$\int_{\rho_{\text{in}}}^{\rho_{\text{out}}} \rho [2SP(\rho) - \Pi_R \eta j^2(\rho)] d\rho = \frac{S}{4\pi} C_3 \alpha_0(\rho_{\text{in}}, \rho_{\text{out}}), \quad \alpha_0 = \frac{\rho_{\text{out}}^2 - \rho_{\text{in}}^2}{2}. \quad (\text{A } 3)$$

Adding (A 2) and (A 3) gives

$$\int_{\rho_{\text{in}}}^{\rho_{\text{out}}} \rho P(\rho) d\rho = \frac{1}{4\pi} \frac{S}{2S + \Gamma} C_3 \alpha_0(\rho_{\text{in}}, \rho_{\text{out}}). \quad (\text{A } 4)$$

Substituting (4.3b) into (A 4) and using (4.5a) reduces the closure condition (A 2) to the following form:

$$4 \frac{1+Z}{\Lambda^2} C_0^{5/2} - \frac{2S}{2S + \Gamma} \alpha_0(\rho_{\text{in}}, \rho_{\text{out}}) C_3 = 0. \quad (\text{A } 5)$$

Appendix B. Explicit solution of the boundary value problem

Using (4.5) and the definition of λ in (4.4), let us rewrite the conditions (4.3) and the closure condition in the following form:

$$I_1(\rho_{\text{out}})C_1 + K_1(\rho_{\text{out}})C_2 = \frac{2}{\Lambda\rho_{\text{out}}} C_0^{3/4}, \quad (\text{B } 1a)$$

$$C_3 - [I_0(\rho_{\text{out}})C_1 - K_0(\rho_{\text{out}})C_2]^2 = 0, \quad (\text{B } 1b)$$

$$I_1(\rho_{\text{in}})C_1 + K_1(\rho_{\text{in}})C_2 = 0, \quad (\text{B } 1c)$$

$$4 \frac{1+Z}{\Lambda^2} C_0^{5/2} - \alpha_0 C_3 + \alpha_{1,1}^2 C_1^2 + \alpha_{2,2}^2 C_2^2 - 2\alpha_{1,2} C_1 C_2 = 0, \tag{B 1d}$$

$$4 \frac{1+Z}{\Lambda^2} C_0^{5/2} - \frac{2S}{2S+\Gamma} \alpha_0 C_3 = 0, \tag{B 1e}$$

where, by denoting the linear operator $2\Delta\Phi(\rho) = \Phi(\rho_{out}) - \Phi(\rho_{in})$,

$$\alpha_0(\rho_{in}, \rho_{out}) = \int_{\rho_{in}}^{\rho_{out}} \rho d\rho \equiv \Delta\{\rho^2\}/2,$$

$$\alpha_{1,2}(\rho_{in}, \rho_{out}) = \int_{\rho_{in}}^{\rho_{out}} \rho I_0(\rho) K_0(\rho) d\rho \equiv \Delta\{\rho^2 [I_0(\rho) K_0(\rho) + I_1(\rho) K_1(\rho)]\}/2,$$

$$\alpha_{1,1}(\rho_{in}, \rho_{out}) = \int_{\rho_{in}}^{\rho_{out}} \rho I_0^2(\rho) d\rho \equiv \Delta\{\rho^2 [I_0^2(\rho) - I_1^2(\rho)]\}/2,$$

$$\alpha_{2,2}(\rho_{in}, \rho_{out}) = \int_{\rho_{in}}^{\rho_{out}} \rho K_0^2(\rho) d\rho \equiv \Delta\{\rho^2 [K_1^2(\rho) - I_1^2(\rho)]\}/2. \tag{B 2}$$

The algebraic system (B1) determines five unknown variables, the coefficients C_j ($j = 0, 1, 2, 3$) and the outer radius of the pinch ρ_{out} (the inner-to-outer radius ratio A and hence $\rho_{in} = A\rho_{out}$ is assumed to be known in the equilibrium state). Then system (B1) may be reduced to the form

$$c_1 I_1(\rho_{out}) + c_2 K_1(\rho_{out}) = 1, \tag{B 3a}$$

$$c_3 - [c_1 I_0(\rho_{out}) - c_2 K_0(\rho_{out})]^2 = 0, \tag{B 3b}$$

$$c_1 I_1(\rho_{in}) + c_2 K_1(\rho_{in}) = 0, \tag{B 3c}$$

$$c_0 - c_3 \alpha_0 - 2c_1 c_2 \alpha_{1,2} + c_1^2 \alpha_{1,1}^2 + c_2^2 \alpha_{2,2}^2 = 0, \tag{B 3d}$$

$$c_0 - \frac{2S}{2S+\Gamma} \alpha_0 c_3 = 0, \tag{B 3e}$$

where the following variable change has been made:

$$c_0 = (1+Z)\rho_{out}^2 C_0, \quad c_1 = \frac{\rho_{out} \Lambda C_1}{2C_0^{3/4}}, \quad c_2 = \frac{\rho_{out} \Lambda C_2}{2C_0^{3/4}}, \quad c_3 = \frac{\rho_{out}^2 \Lambda^2 C_3}{4C_0^{3/2}}. \tag{B 4}$$

The subsystem (B3b)–(B3d) of the system (B3) may be reduced to a system of two linear equations with respect to c_1^2 and c_3 :

$$\chi_0 c_3 - \chi_1 c_1^2 = 0, \tag{B 5a}$$

$$\chi_2 c_3 - \chi_3 c_1^2 = 0, \tag{B 5b}$$

where

$$\chi_0(\rho_{in}) = K_1^2(\rho_{in}), \quad \chi_1(\rho_{in}, \rho_{out}) = I_0(\rho_{out}) K_1(\rho_{in}) + I_1(\rho_{in}) K_0(\rho_{out}),$$

$$\chi_2(\rho_{in}, \rho_{out}) = \frac{\Gamma}{\Gamma+2S} K_1^2(\rho_{in}) \alpha_0,$$

$$\chi_3(\rho_{in}, \rho_{out}) = K_1^2(\rho_{in}) \alpha_{1,1} + I_1^2(\rho_{in}) \alpha_{2,2} + 2I_1(\rho_{in}) K_1(\rho_{in}) \alpha_{1,2}.$$

The system (B 5) has a non-trivial solution at zero discriminant

$$D(\rho_{\text{in}}, \rho_{\text{out}}; S) \equiv \chi_0 \chi_3 - \chi_1 \chi_2 = 0. \quad (\text{B } 6)$$

Then, assuming the outer radius of the pinch ρ_{out} to be found from the eigenvalue equation (B 6) for any given A ($0 < A < 1$) and omitting one of the equations, e.g. (B 3d) from the subsystem (B 3b)–(B 3e), the rest equations (B 3) provide for expressions for the coefficient c_k ($k = 0, 1, 2, 3$):

$$c_0 = \frac{2S}{2S + \Gamma} \frac{\chi_1}{\Delta^2} \alpha_0, \quad c_1 = \frac{K_1(\rho_{\text{in}})}{\Delta}, \quad c_2 = \frac{I_1(\rho_{\text{in}})}{\Delta}, \quad c_3 = \frac{\chi_1}{\Delta^2}, \quad (\text{B } 7)$$

where $\Delta(\rho_{\text{in}}, \rho_{\text{out}}) = I_1(\rho_{\text{out}})K_1(\rho_{\text{in}}) + I_1(\rho_{\text{in}})K_1(\rho_{\text{out}})$. Then (B 4) provide expressions for the unscaled coefficient C_k ($k = 0, 1, 2, 3$):

$$C_0 = \frac{c_0}{(1 + Z)\rho_{\text{out}}^2}, \quad C_1 = \frac{2c_1 C_0^{3/4}}{\Lambda \rho_{\text{out}}}, \quad C_2 = \frac{2c_2 C_0^{3/4}}{\Lambda \rho_{\text{out}}} c_2 C_0^{3/4}, \quad C_3 = \frac{4c_3 C_0^{3/2}}{\Lambda^2 \rho_{\text{out}}^2}. \quad (\text{B } 8)$$

Substituting (B 8) into (4.5) provides explicit expressions for the radial distributions of temperature, magnetic field, current, and pressure.

References

- Bud'ko, A. B., Kravchenko, Yu. and Uby L. 1994 Exact solutions of the dissipative screw-pinch problem. *Plasma Phys. Control. Fusion* **36**, 833–853.
- Coppins, M., Culverwell, I. D. and Haines, M. G. 1988 Time dependent Z-pinch equilibria. *Phys. Fluids* **31**, 2688–2694.
- Coppins, M., Chittenden, J. P. and Culverwell, I. D. 1992 Self-similar Z-pinch equilibria in the unmagnetized regime, and their role in pinch evolution. *J. Phys. D: Appl. Phys.* **25**, 178–187.
- Davara, G., Gregorian, L., Kroupp, E. and Maron, Y. 1998 Spectroscopic determination of the magnetic-field distribution in an imploding plasma. *Phys. Plasmas* **5**, 1068–1076.
- Deeba, F., Ahmed, K., Haseeb, M. Q. and Mirza, A. M. 2005 Finite-effect on the dynamics of double gas-puff staged pinch. *Phys. Scr.* **72**, 399–403.
- Gregorian, L., Bernshtam, V. A., Kroupp, E., Davara, G. and Maron, Y. 2003 Use of emission-line intensities for a self-consistent determination of the particle densities in a transient plasma. *Phys. Rev. E* **67**, 016404.
- Gregorian, L., Kroupp, E., Davara, G., Fisher, V. I., Starobinets, A., Bernshtam, V. A., Fisher, A. and Maron, Y. 2005a Electron density and ionization dynamics in an imploding z-pinch plasma. *Phys. Plasmas* **12**, 092704.
- Gregorian, L., Kroupp, E., Davara, G., Starobinets, A., Fisher, V. I., Bernshtam, V. A., Ralchenko, Yu. V., Maron, Y., Fisher, A. and Hoffmann, D. H. H. 2005b Electron-temperature and energy-flow history in an imploding plasma. *Phys. Rev. E* **71**, 056402.
- Kroupp, E., Osin, D., Starobinets, A., Fisher, V., Bernshtam, V., Maron, Y., Uschmann, I., Forster, E., Fisher, A. and Deeney C. 2007 Ion-Kinetic-Energy Measurements and Energy Balance in a Z-Pinch *Phys. Rev. Lett.* **98**, 115001.
- Kruskal, M. and Schwarzschild, M. 1954 Some instabilities of completely ionized plasma. *Proc. Royal Soc. London A* **223**, 348–360.

- Lifshits, E. M. and Pitaevskii, L. P. 1981 *Physical Kinetics*. Oxford: Pergamon Press.
- Ryutov, D. D., Derzon, M. S. and Matzen, M. K. 2000 The physics of fast Z pinches. *Rev. Mod. Phys.* **72**, 167–223.
- Shtemler, Y. M. and Mond, M. 2005 Asymptotic self-similar solutions for thermally isolated Z-pinches. *J. Plasma Phys.* **71**, 267–287.
- Shtemler, Y. M. and Mond, M. 2006 Nonlinear evolution of perturbations in Hall MHD Z-pinch plasmas. *J. Plasma Phys.* **72**, 699–710.